

Shock Propagation Effects in Multilayer Assembly Including a Liquid Phase

Judith BOURGUILLE¹, Luca BERGAMASCO², Gilles TAHAN¹,
Daniel FUSTER², Michel ARRIGONI^{1,a*}

¹ENSTA Bretagne / IRDL FRE n°3744, 2 rue François Verny, 29806 Brest Cedex 09, France

²Institut Jean Le Rond D'Alembert, Université Pierre et Marie Curie, Paris, France

^amichel.arrigoni@ensta-bretagne.fr

Keywords: Cavitation, Light weight armours, Protection, Laser induced shock waves

Abstract. During a ballistic impact, the protective material that plays the role of armour has to dissipate the kinetic energy in order to limit the projectile penetration in the target. Our aim is to emphasize on the role played by a liquid-filled system on the impact energy mitigation due to cavitation inception and later bubble expansion. To observe this, small scale experiments have been carried out on a three layers sample (Aluminium-Water-PMMA) submitted to shock waves induced by laser impact applied on the Al face. Rapid camera visualizations allow reproducing, at small scale, the effects of projectiles on armours for various monitored impact energies. We observe the formation of bubbles for sufficiently intense impacts due to traction effects in the water caused by the multiple reflections of waves within the sample. The cavitation threshold of water under dynamic loading is then experimentally investigated for two samples: one with 600 µm thick Al / 400 µm of water and 3 mm of PMMA, the other with 1000 µm thick Al / 1600 µm of water and 3 mm of PMMA. Using dimensional analysis, we show that the energy taken during the process of inception and bubble expansion becomes more important as the energy of the impact increases.

Introduction

Protection devices against intense shocks are mainly based on energy absorption by strain (steel plates, composites) [1] or compaction (foams) [2, 3]. Recently, fluid phase have been introduced in shielding for procuring a benefit against penetration by the use of “shear thickening fluids” [4]. One of the properties of fluids is their capability to cavitate, this process being a very dissipative mechanism. Indeed, cavitation is a phase transition from liquid to gas, which occurs when a negative pressure is applied at constant temperature, consuming energy in the process and changing the mechanical properties of the medium in which waves propagate. Cavitation under ballistic impact has been observed on ballistic gels as human simulating [5, 6] as they provide a better understanding of post-traumatic injuries following ballistic impact on light protections.

An application involving cavitation media in the field of protection is presented by Schimizze [7]. The concept is dedicated to protecting against the blast effects of improvised explosive devices and is based on a lightweight structural shield containing a fluid cavity that may be water, glycerin or an airgel. Their experience consisted of transmitting a shock of amplitude 5 bars and a hundred microsecond duration, of blast wave type, through a fluid sandwiched between two plates. Transmitted pressure was measured on the other side of the plate. The results obtained by Schimizze [7] show that the pressure peak transmitted beyond the shield is reduced by half when cavitation process occurs.

Water penetrations by ballistic impact are subjected to Hydrodynamic RAM effects when the bullet penetrates the water volume. An analytical model was developed by Lee et al. to predict water cavitation after high speed projectile impact [8]. Recently, Deletombe described the HRAM provoked by the penetration of a 7.62 mm bullet in a large pool as well as in a fluid filled tank [9]. T. Fourest et al. expanded this study [10] and determined corrections parameters for the Rayleigh-Plesset equation that describes the gas bubble pulsation in the fluid volume. Those works are focused on the description of the Hydrodynamic Ram process and its mechanical loading on its

environment. In the present study we are interested in the possibility of a shield using fluid cavitation to dissipate energy from a ballistic impact, which from our best knowledge of the literature was never done.

It should be emphasized that cavitation is a phenomenon of phase change within a liquid, due to a depression going below the threshold of saturating vapour pressure of the liquid. When considering impact, it comes first in mind a compression wave of high intensity. This wave propagates from the impact zone to the facing free surface, often referred to as the back face. By the play of wave reflections and transmissions governed by acoustic impedance mismatch between each propagation medium, when the shock wave reaches the back surface, it is reflected as a fan of expansion waves that propagate towards the impact zone. On the way back, these releases cross the releases of the unloading of the impact process, which are at least the lateral releases propagating from the perimeter of the impact, to the center, propagating towards the back face. The crossing of release waves has the notorious effect of generating traction in the propagation medium (spallation in solids). These effects were studied before [11]. When the liquid is subjected to this traction, it cavitates, and some gas bubbles are then visible. This cavitation process consumes energy by several effects [12]. The gas bubble will follow a dynamic and enter the pulsation regime by compressing itself (heating and thus heat dissipation) and expanding several times (dissipation by viscosity) in a confined medium (within a cavity or a pore). This situation has been described by Fourest [13]. Cavitation is enhanced if the liquid medium is confined between two plates of high acoustic impedance with respect to that of the liquid, in particular that of the back face (in general, steel). The bubble exerts a thrust on walls, which will be directed towards the front face due to confinement (generally aluminium). The momentum applied on it thus opposes to the advance of the projectile. For a better understanding of bubbles' behaviour, we used a simplified Rayleigh-Plesset equation to model them [14]. Bergamasco and Fuster obtained phase diagrams for the bubble oscillation regimes [15]. This theoretical linear analysis allows us to distinguish the conditions under which different mechanisms control the response of bubbles against an external pressure perturbation. In particular, they show that, even at very low frequencies, transient heat diffusion in the liquid and mass diffusion inside the bubble can play an important role on its dynamic response.

We want to bring some experimental evidences of this penetration mitigation by the use of laboratory scale experiments relying on laser induced shock waves instead of bullet impacts. The advantage of using a laser driven shock waves is to be able to access pressure levels up to 5 to 6 GPa, while being able to be tuned. These loading conditions are not exactly those induced by a ballistic impact, but they allow a laboratory study and the detection of the expected phenomena. In the present article, after a brief state of the art, the experimental setup utilized for this study is presented in paragraph 2. It describes the setup and the target. In paragraph 3 some results are shown, it allows us to obtain the life duration of cavitation bubbles. The following paragraph develops a discussion of obtained results. A conclusion and perspectives are then proposed.

Experimental Setup

Set-up. The laser source of ENSTA Bretagne was used as a shock generator. It is a Quanta Ray Pro 350-10 manufactured by Spectra-Physics. It delivers a pulse of $\tau = 10$ ns duration and a maximal energy (E_{max}) of 3.7 J at $\lambda = 1064$ nm. The laser beam is focused on the horizontal sample using a lens and a mirror at 45° (see Figure 1). The laser energy can be adjusted using an attenuator of energy of the beam laser. It can also be monitored by adjusting the spot size, which is an elliptical of 4 mm diameter in average obtained by focusing the beam with a convex 200 mm focal length.

Laser induced shock wave can be obtained by focusing a high energy laser delivering a short pulse on a reduced surface. The laser matter interaction in ablation regime occurs when the density of power deposited on the irradiated surface is above about 0.5 GW/cm^2 [16]. Ablation of the material by the laser generates a plasma expansion that transmits a compression wave in the target, like an explosion. This wave propagates within the target. When it reaches the rear face of the sample, rarefaction waves are, in our case, reflected. Those will meet others rarefaction waves

which are due to the unloading of the process of impact and create traction (negative pressure) in the material. More details on this can be found in [16]. Two types of laser shock were induced. The first one is to shock directly on the sample surface, which will be called “non confinement” in this article. The second one will be called “water-confined”: when using a thin water layer over the sample, the plasma expansion is constrained, what results in increasing the pressure (from 5 to 10 times) and the pulse duration (from 2 to 3 times) [17, 18].

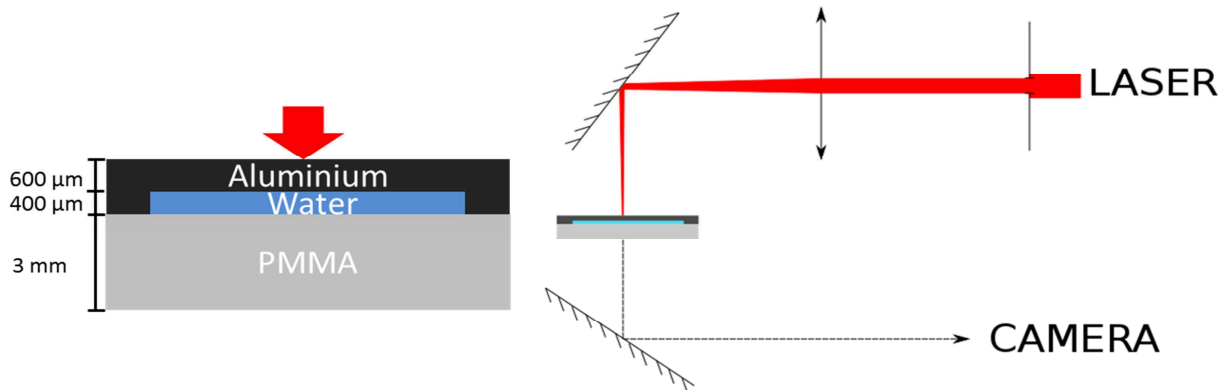


Fig. 1 On the right, scheme of the experimental setup. In red the laser path of the shock generator is visualised passing through a lens and a mirror at 45° and focused on the sample. On the left, cross-sectional view of the sample A. Sample B is similar with different thicknesses for aluminium and water.

Measurement of the incident laser energy and focal spot size were made for each experiment. Only one shot per Energy level was performed but the repetitivity of the laser source was evaluated with a Gentec Maestro® Joulemeter over 100 shots per energy level. The standard deviation of the measured energy was of the order of 2.5 %. A 45° mirror was placed below the sample to observe cavitation effects inside the water layer of our sample. Imaging was done by filming with a Photron FASTCAM SA-X2 type 1080K-M4, at 200000 frames per second (an image every $5 \mu\text{s}$).

Samples. To investigate the effects of water and aluminium layers thicknesses on cavitation, two samples were designed. In the first case (called later sample A, presented in Figures 1 and 2) a $600 \mu\text{m}$ aluminium layer and $400 \mu\text{m}$ of water layer were used. The second sample (sample B) had a $1000 \mu\text{m}$ aluminium layer and $1600 \mu\text{m}$ water. In both cases, to allow visualisation of the phenomenon, a 3 mm PMMA layer is backing the water layer, even though it is definitely not a realistic material for armour. To put water inside the sample, a groove of the desired dimensions inside the aluminium piece was machined as shown in Figure 2. Then, the PMMA plate, drilled of two small holes, was glued on the aluminium part. A syringe was inserted through one hole to fill in the air volume with water into the sample, while the other hole permits the escape of trapped air. An adhesive tape crystal was finally put to seal the holes.

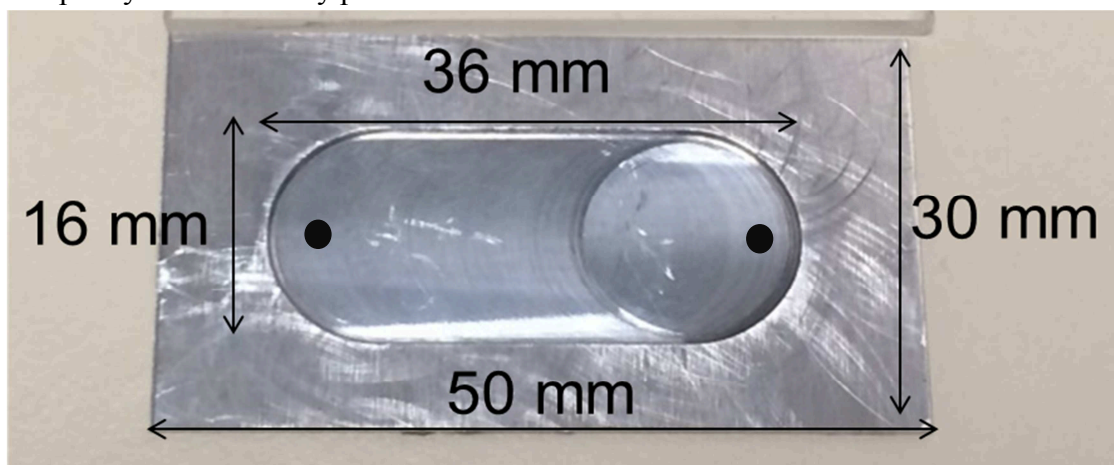


Fig. 2 Dimensions of the groove created for the water in the aluminium piece of the sample A. The black circles correspond to emplacements of holes in the PMMA part.

Experimental Results

For the sample A, depending of the deposited laser energy, cavitation was observed for both non confined and water-confined laser shocks. In general, it was visible under the form of bubbles cloud between 5 to 10 μs after laser impacts on the aluminium part bearing the shock wave. Figures 3 show pictures taken with the camera at 0 μs (Images A and C) and 40 μs (Images B and D) for an experiment without confinement at a laser energy of 70 % E_{max} (Images A and B) and one water-confined at 50 % E_{max} (Images C and D).

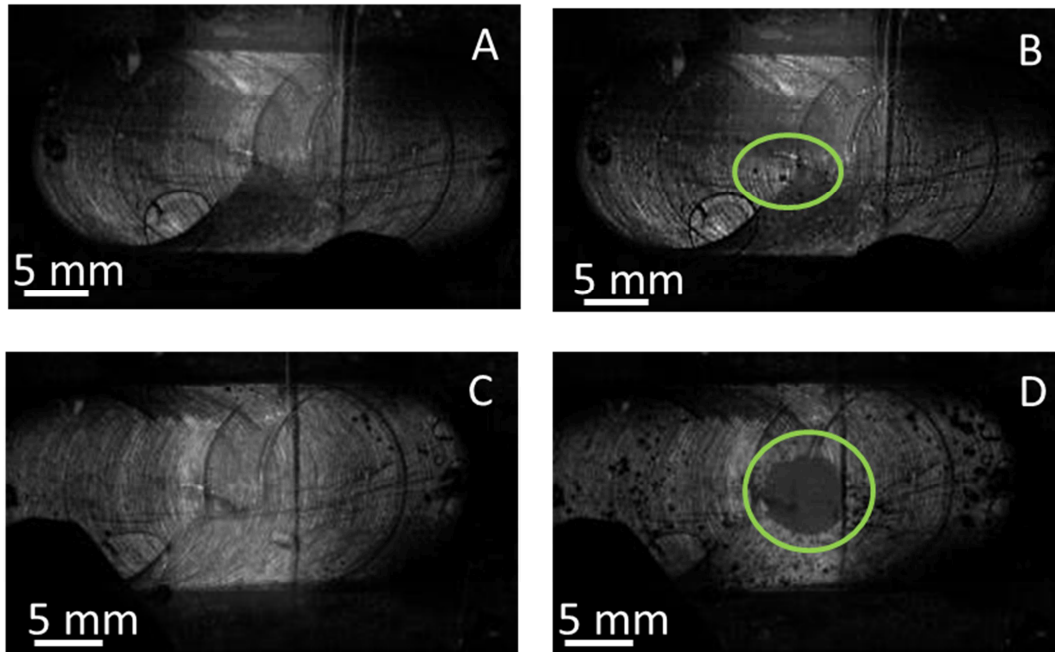


Fig. 3 Images recorded by the Photron FASTCAM SA-X2: A and B are of an experiment at a laser energy of 70 % E_{max} . Images C and D are of one at 50 % E_{max} but water-confined. Both images A and C are at $t = 0 \mu\text{s}$, at the impact laser on the aluminium part of the sample. Images B and D are at $t = 40 \mu\text{s}$. We can see isolated bubbles for B and an important cloud of bubbles in D, in the green circles.

In the first case, at 70% E_{max} without confinement, small isolated bubbles (Fig. 3B), while in the second test (50% E_{max} but in confined geometry, that is to say with more pressure), a cloud of bubbles is observed (Fig. 3D). In general, when cavitation occurs in non-confined experiments, the bubble disappears and then briefly reappears for about 15 μs . This particular pattern was observed once at the lowest energy laser for water-confined experiments, for all the others, the bubble cloud pulsated at a frequency of about 45 μs . Lifetimes of bubbles in both situations were measured by picture analysis with ImageJ® [19]. For non-confined experiments, a linear behaviour is seen as soon as cavitation occurs (for the lowest laser energies, no cavitation is observed). As laser energy increases, the lifetime of bubbles does too (fig. 4). For laser energy, we took 5% of deviation of the value E_{max} and plus/minus 5 μs for the measured lifetime.

An important difference between both configurations (with and without confinement) is seen for the lifetime of the cloud of bubbles. Bubbles clearly appear already at the lowest laser energy (10 % E_{max}) and measures of lifetime of the cloud seem indicate a threshold value (green triangles, fig. 4). Moreover, the duration of the cavitation is higher than those of the non-confinement experiments (blue diamonds, fig. 4). This is a consequence of the magnification of the shock wave and then its consequent tensile wave when reflected at the interfaces of the target, reaching the cavitation threshold at lower energy in water confined geometry. The lifetime is not linear any more with respect to the energy, as the energy is not linear to the generated pressure in water confined geometry.

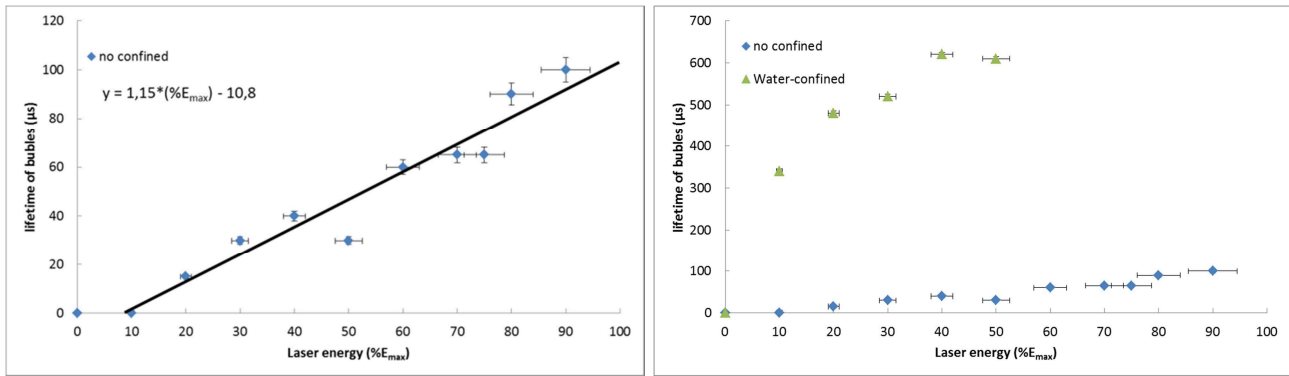


Fig. 4 On the left, life time of bubbles with respect to the laser confinement and energy. In blue is the lifetime of the longest bubble. After the phenomenon occurs at 20 % E_{max} , a linear behaviour is seen. On the right, life time of bubbles with respect to the laser confinement and energy, with the addition of the lifetime of the cloud of water-confined experiments (green triangles).

Contrary to sample A, for the sample B, we could not determine if non confinement laser shocks induced cavitation as we did not observe clearly bubbles. Preliminary observations seem to indicate that, like in the case of water-confined shots on sample A, the presence of a threshold both in the quantity of bubbles that cavitation generates and in the lifetime of the cloud of bubbles. Apparition of bubbles at a later time is noticed on sample B, thicker. It is also noticeable that for lowest laser energy, there is a similar behaviour of isolated bubbles in sample B as observed with sample A at low energy and at highest energy. The behaviour of bubble clouds for both samples also shows some similarities.

For a thicker layer of aluminium and water, bubbles are more scattered in the sample and are free to move and grow inside it.

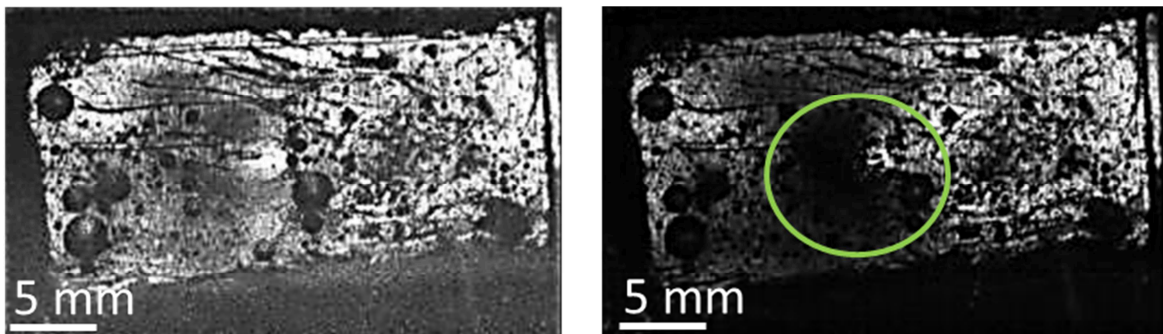


Fig. 5 Water-confined laser shock at 90 % E_{max} for the sample B. Left: sample B at $t = 0 \mu\text{s}$. Right: laser shock propagated inside the sample and bubbles (inside green circle) appeared, $t = 40 \mu\text{s}$.

Discussion

Laser shock induced cavitation inside samples has been observed by rapid imaging at 200000 frames per second. Those results show that they are at least two different behaviours for the bubbles induced by laser induced shockwave: One at lowest energies as free pulsating bubbles and one at highest energies as pulsating bubble cloud. The lifetime of bubbles depends of laser energy deposited for the shock creation. The lifetime of bubbles increases with laser energy and seems to reach a threshold at higher energies, or at least to not increase linearly with energy. This behaviour is explained by the dependence of the generated shock pressure that also governs the tensile stress intensity and duration in addition to the enlargement of the spatial profile. However, this also seems to be a difference between non confinement and water-confined experiments: the later achieved more rapidly long lifetime of bubbles. It points out a threshold for cavitation as not all laser energies generate cavitation this threshold is around 10% of E_{max} , which gives a peak pressure of about 150 MPa with duration of 20 ns at half maximum. In both cases pulsation were determined by video analysis.

Post-treatment of pictures is complicated by the sample configuration and laser shock, in particular small deformation of aluminium plate. For image processing, an image at rest (before shot) was subtracted to the image of interest to keep only the pixel difference that reveals bubble apparitions and eventually water displacement. A quantity of white pixels is then obtained by thresholding the picture, corresponding to the bubbles.

Figure 6 shows the evolution of the diameter of the bubbles in function of time, in cases of water confined measurement. As more energy is given to the system, bubbles diameter and longevity increase. Creation and expansion of the bubbles are faster than collapse of said bubbles.

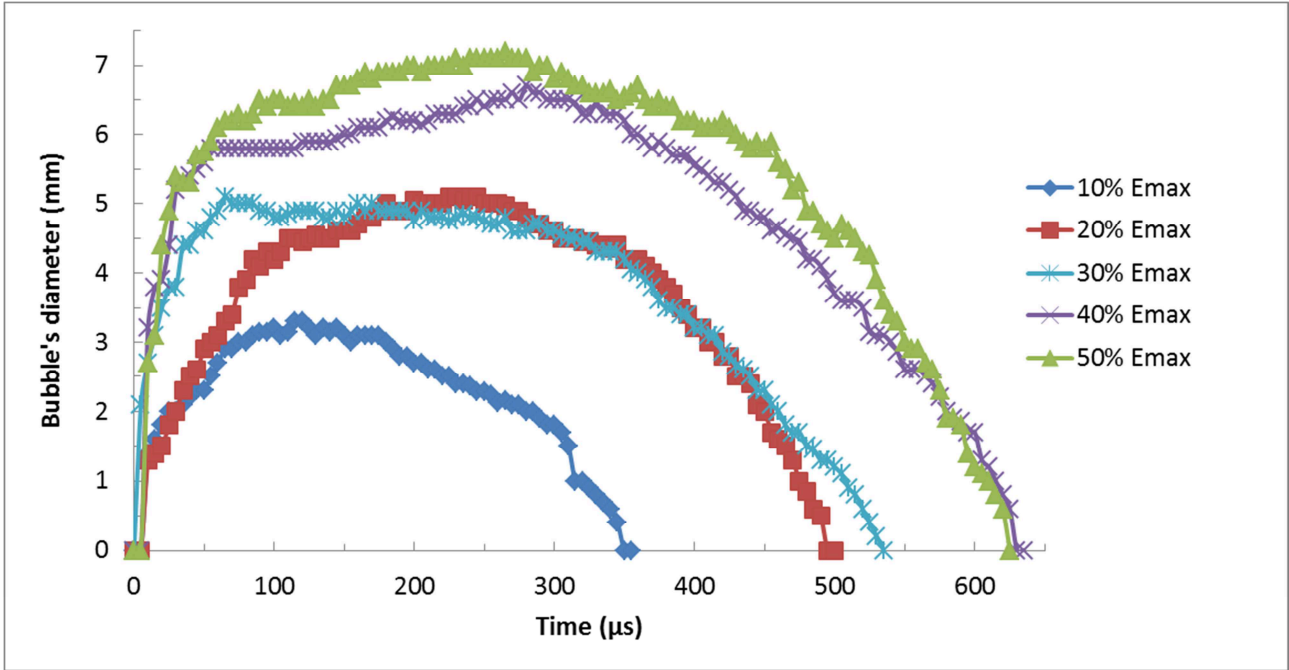


Fig. 6 Graphic of the dependence of bubbles diameter against time in water confined experiments.

In order to gain more understanding on the dynamic response of the expanding/collapsing bubbles we propose a simple model based on a variation of the classical Rayleigh-Plesset equation used to investigate the response of bubbles. The equation based on the solution on cylindrical coordinates assuming a Poiseuille flow profile in the perpendicular direction. The well-known singular behaviour of the resulting equation for the pure 2D case can be solved by assuming that the velocity profiles decays as (Eq. 1):

$$u(r) = \dot{R} \left(\frac{R}{r} \right)^\alpha, \quad (1)$$

where $\alpha=1$ in a pure 2D case. In reality, the presence of other bubbles, the deformation of the material or possible leaks in the system makes $\alpha>1$. Note that for a 3D spherical bubble in a free liquid $\alpha=2$, then, we expect in a real system α to take values $1<\alpha<2$.

The non-dimensional version of the Rayleigh-Plesset equation derived under these conditions is (Eq. 2):

$$R\ddot{R} + \frac{2\alpha-1}{2}\dot{R}^2 = (p_l(r=R) - p_\infty) \frac{t_{Rayleigh}^2}{R_0^2} - \frac{Re^{-1}}{\alpha-1} R\dot{R}, \quad (2)$$

where R_0 is the characteristic bubble radius, the characteristic time is $t_{Rayleigh} = R_0\sqrt{\rho/p_0}$, and the Reynolds number is defined as $Re = \frac{\rho h^2/t_{Rayleigh}}{\mu}$, h being the thickness of the water layer.

It is interesting to investigate the Rayleigh collapse time t_c obtained assuming that when the bubble reaches its maximum radius, the internal pressure is much smaller than the reference pressure, which is assumed to be constant. In this case, for a 3D bubble, $\frac{t_c}{t_{Rayleigh}} = 1$. Figure 7 shows the numerical solution of the nondimensional collapse time as a function of α and the Reynolds

number. The numerical solution reveals that the collapse time is predominantly function of the Reynolds number (the influence of α is almost negligible). As expected, an asymptotic limit of the Rayleigh collapse time for large values of the Reynolds number is reached. For the experiments reported here $Re > 2000$ and therefore we expect $R_0/t_c \approx \sqrt{p_0/\rho}$, where t_c corresponds to the half of the lifetime of the bubble. The data obtained in the experimental conditions where large bubbles are observed reveal that R_0/t_c remains approximately constant and equal to 10 m/s for all conditions. This value corresponds to $p_0=1\text{atm}$.

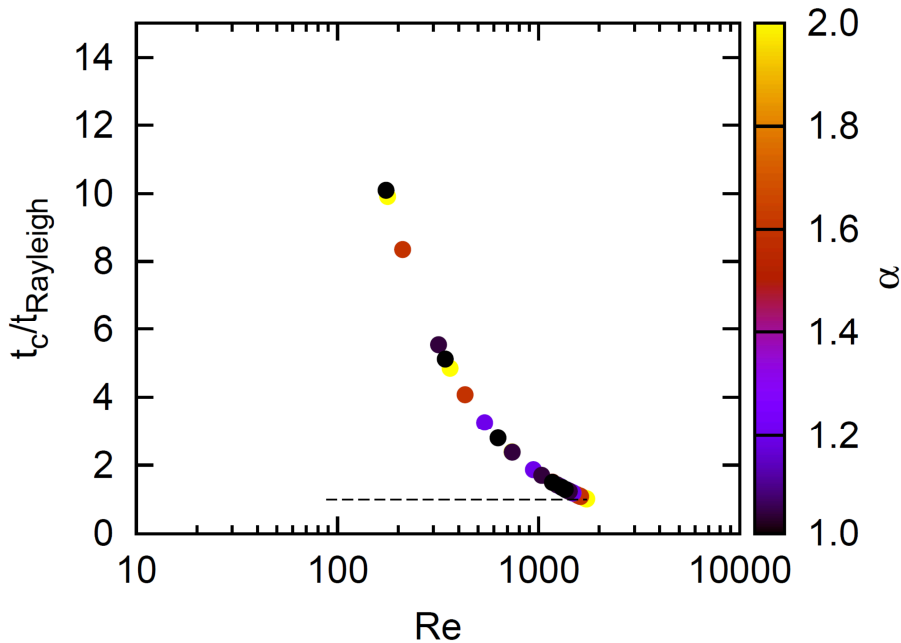


Fig. 7 Experimental measurement of the Rayleigh collapse time as a function of the parameter α and Reynolds.

Another important point to be considered is the energy taken by the bubble during its expansion. In a first approximation, this energy can be obtained as $E=p_0 \pi R^2 h$. Using the Rayleigh collapse time to express R as a function of t we conclude that the energy absorbed by the bubble during the expansion scales with t_c^2 . Given that the collapse time is shown experimentally to scale linearly with the input laser energy, it is clear that the energy taken by the process of bubble expansion grows faster than the input energy. This implies that the process of cavitation inception and bubble expansion becomes more important when the input energy increases.

Conclusion and Perspectives

Conclusions. We were trying to demonstrate the feasibility of a water-filled shield, using cavitation to dissipate energy from bullets. We developed a system Aluminium-Water-PMMA in order to observe and quantify, at laboratory scale, cavitation of water after a laser shock. We obtained experimental evidences that cavitation occurs in our water-filled system after the passage of laser induced shock waves. This experimental setup also allowed finding a cavitation threshold under shock conditions. We could observe bubbles formation, expansion and collapse and measure their lifetime and diameter. We obtained a good correlation between increase of laser energy and increase of lifetime and diameter. Moreover, using a simple model, Rayleigh-Plesset equation, we obtain that cavitation inception and bubble expansion increase with increase of laser energy provided to the system.

Perspectives. We now have a process to determine conditions of cavitation and behaviour of bubbles. For a better understanding of this phenomenon, experiments with others thicknesses for both aluminium and water parts and other liquids are considered. We were able to obtain cavitation of water contained between aluminium and PMMA. To verify the possibility of using this as an

armour, we will replace PMMA by steel. The use of heterodyne velocimetry system would allow us to confirm bubble's formation inside the system as we could measure free surface velocities of aluminium plate and see how the heterodyne velocimetry signal reacted to formation of bubbles. Using those measurements we could compare behaviour of the water inside an aluminium-PMMA sandwich and an Aluminium-steel one which correspond to actual shield as steel is one of the commonly material used for protection. In addition, by using Finite Element Analysis (FEA) tools we could be able to determine the stress history at the origin of the cavitation. It would also allow determining the mechanical load transmitted to a backing plate and thus to evaluate the dissipated energy and the protection efficiency.

Acknowledgements

The authors would like to thanks ANR for the grant n° 15-ASTR-0026-02 that support the CACHMAP project. The authors would like to thank the staff of ENSTA-Bretagne, in particular for the technical support, as well as Pierre Ginsburger and Maxime Voisin, MSc students, who helped on this project.

References

- [1] R. Laible, (Ed.). *Ballistic materials and penetration mechanics* (Vol. 5). Elsevier (2012)
- [2] B. A. Gama, T. A. Bogetti, B. K. Fink, C. J. Yu, T. D. Claar, H. H. Eifert and J. W. Gillespie Jr, "Aluminum foam integral armor: a new dimension in armor design", *Composite Structures* 52(3), 381-395 (2001)
- [3] L. Aktay, A. F. Johnson and M. Holzapfel, "Prediction of impact damage on sandwich composite panels", *Computational Materials Science* 32(3), 252-260 (2005)
- [4] R. G. Egres Jr, Y. S. Lee, J. E. Kirkwood, K. M. Kirkwood, E. D. Wetzel and N. J. Wagner, "Liquid armor: protective fabrics utilizing shear thickening fluids", in *Proceedings of the 4th International Conference of Safety and Protective Fabrics, Pittsburg, PA* (2004, October)
- [5] L. Liu, Y. Fan and W. Li, "Viscoelastic shock wave in ballistic gelatin behind soft body armor", *Journal of the mechanical behaviour of biomedical materials* 34, 199-207 (2014)
- [6] D.S. Cronin, M.J. Worswick, A.V. Ennis, D. Bourget, K. V. Williams and G. Pageau, "Behind Armour Blunt Trauma for ballistic impacts on rigid body armour", in *19th Int. Symp. Ballistics, International Ballistics Society, Interlaken, Switzerland* (2001, May)
- [7] B. Schimizza, S.F. Son, R. Goel, A.P. Vechart and L. Young, "An experimental and numerical study of blast induced shock wave mitigation in sandwich structures", *Applied Acoustics*, 74(1), 1-9 (2013)
- [8] M. Lee, R.G. Longoria, and D.E. Wilson, "Cavity dynamics in high-speed water entry", *Physics of Fluids* 9(3), 540-550 (1997)
- [9] E. Deletombe, Fabis J, Dupas J, Mortier "Experimental analysis of 7.62 mm hydrodynamic ram in containers", *J Fluids Struct* 37, 1-21 (2013)
- [10] T. Fourest, J.-M. Laurens, E. Deletombe, J. Dupas and M. Arrigoni, "Analysis of bubbles dynamics created by hydrodynamic ram in confined geometries using the rayleigh-plesset equation", *International Journal of Impact Engineering* 73, 66-74 (2014)
- [11] M. Boustie, L. Berthe, T. De Ressaiguiet and M. Arrigoni, "Laser shock waves: fundamentals and applications", in *Proc. 1st Int. Symp. On Laser Ultrasonics: Science, Technology and Applications* (2008, July)
- [12] H. Grandjean, N. Jacques and S. Zaleski, "Shock propagation in liquids containing bubbly clusters: a continuum approach", *J. Fluid. Mech.* 701, 304h332 (2012)

-
- [13] T. Fourest, “Développement et validation de modèles de dynamique de bulles confinées pour la simulation du coup de bélier hydrodynamique dans les réservoirs de carburants”, Thesis (2015)
- [14] D. Fuster and T. Colonius, “Modelling bubble clusters in compressible liquids”, *Journal of Fluid Mechanics* 688, 352-389 (2011, December)
- [15] L. Bergamasco and D. Fuster, “Oscillation regimes of gas/vapor bubbles”, *International Journal of Heat and Mass Transfer* 112, 72–80 (2017)
- [16] M. Boustie, J.P. Cuq-Lelandais, C. Bolis, L. Berthe, S. Barradas, M. Arrigoni, and M. Jeandin, “Study of damage phenomena induced by edge effects into materials under laser driven shocks”, *Journal of Physics D: Applied Physics* 40 (22), 7103 (2007)
- [17] R. Fabbro, J. Fournier, P. Ballard, D. Devaux and J. Virmont, “Physical study of laser-produced plasma in confined geometry”, *J. Appl. Phys.* 68 (2), 775–784 (1990)
- [18] L. Berthe, R. Fabbro, P. Peyre, L. Tollier and E. Bartnicki, “Shock waves from a waterconfined laser-generated plasma”, *J. Appl. Phys.* 82 (6), 2826–2832 (1997)
- [19] C. A. Schneider, W.S. Rasband and K. W. Eliceiri, “NIH Image to ImageJ: 25 years of image analysis”, *Nature methods* 9 (7), 671 (2012)